Paper “as accepted for publication" in 2023 Proceeding of the 45th Annual International Conference of the IEEE Engineering in Medicine and Biology Society (EMBC), July 24-27, 2023. Sydney (Australia).
Published version: https://dx.doi.org/10.1109/EMBC40787.2023.10340338

Towards the definition of Microstates of the Cortical Brain-Heart Axis

Vincenzo Catrambone, *Member*, *IEEE*, and Gaetano Valenza, *Senior Member*, *IEEE*

***Abstract*— Brain microstates are defined as states with quasi-stable scalp activity topography and have been widely studied in literature. Whether those states are brain-specific or extend to the body level is unknown yet. We investigate the extension of cortical microstates to the peripheral autonomic nerve, specifically at the brain-heart axis level as a functional state of the central autonomic network. To achieve this, we combined Electroencephalographic (EEG) and heart rate variability (HRV) series from 36 healthy volunteers undergoing a cognitive workload elicitation after a resting state. Our results showed the existence of microstates at the functional brain-heart axis with spatio-temporal and quasi-stable states that exclusively pertained to the efferent direction from the brain to the heart. Some of the identified microstates are specific for neural or cardiovascular frequency bands, while others topographies are recurrent over the EEG and HRV spectra. Furthermore, some of the identified brain-heart microstates were associated with specific experimental conditions, while others were non-specific to tasks. Our findings support the hypothesis that EEG microstates extend to the brain-heart axis level and may be exploited in future neuroscience and clinical research.**

I. Introduction

Cortical brain dynamics measured by electroencephalography (EEG) exhibit transient quasi-stable states that are manifested through specific scalp topographies temporally close to the peaks of the global field potential (GFP) [1], [2]. It is possible to consistently identify a limited amount of prototypical microstates, repeatedly appearing in multiple brain dynamics. These states have been referred to as scalp/EEG microstates and are thought to be the building blocks of spontaneous conscious mental processes [3].

The occurrence of microstates found its physiological bases on the current, well-established understanding that brain functions result from intense parallel processing in diffused and distributed brain networks [4], [5]. Most studies investigating the relationship between microstates and brain activity have focused on the resting state networks, specifically the default mode network [1]. Recent research has found links between microstate dynamics and other functional cognitive activities [1], as well as physiological [2] and pathological [6] conditions.

Authors are with the NeuroCardiovascular Intelligence lab, Bioengineering and Robotics Research Center E. Piaggio & Department of Information Engineering, School of Engineering, University of Pisa, Pisa, Italy Correspondence to: vincenzo.catrambone@ing.unipi.it

The research leading to these results has received partial funding from the European Commission H2020 Framework Programme under Grant No. 101017727 of the project EXPERIENCE, from the Italian Ministry of Education and Research (MIUR) in the framework of the FoReLab project (Departments of Excellence), and of the PNRR Tuscany Health Ecosystem (cod. ECS00000017 - CUP I53C22000780001).

Numerous brain regions have been linked to microstate dynamics, including the insula, thalamus, amygdala, anterior cingulate cortex, and others [7], [8]. Of note, these brain regions also belong to the so-called central autonomic network (CAN) [9]. CAN encompasses brain areas functionally linked to sympathetic and parasympathetic nerves activity and is involved in the functional brain-heart interplay (BHI) [9]. BHI is directional, dynamic, and diffuse over the brain and comprises autonomic-central nervous system communications through anatomical, biochemical, and electrical links. Combined analysis of EEG and heart rate variability (HRV) series has shown that healthy BHI variations occur in response to various events, such as emotion perception [10], alternating sleep stages [11], cognitive load [12], and autonomic maneuvers [13]. Despite the aforementioned evidence achieved by BHI analysis, some aspects remain to be investigated. In particular, functional BHI has mainly been studied at an EEGelectrode specific level, thus identifying the functional coupling between EEG oscillations of specific locations, and heartbeat oscillations, without considering a nervous-system-wise level of interplay.

While brain activity is studied as interaction of embedded networks, and presence of EEG microstates has been established in brain regions belonging to the CAN, the existence of microstates at the broader BHI level remains unclear. This study hypothesizes that microstates extend to the brain-heart domain and examines the functional connections between the brain and heart during rest and in response to cognitive stress. To test this hypothesis, a novel processing pipeline was developed to estimate channel-specific and time-resolved functional BHI and treated as BHI-GFP. If microstates extend to the brain-heart level, the BHI-GFP series should be able to explain the overall variance of the scalp BHI and exhibit meaningful changes in response to experimental elicitation. Since EEG microstates are commonly considered as “atoms of thoughts”, their extension to the body level, would represent the definition of BHI microstates as “atoms of interoception”.

Next, we report details on the methodology and experimental dataset related to cognitive workload stress using multiple mental arithmetic tasks (MA) [14].

II. Materials and Methods

A schematic representation of the analysis pipeline implemented in this study is depicted in figure 1.

A. Experimental Dataset and Signal Preprocessing

The "EEG During Mental Arithmetic Tasks" dataset [14] was selected from the Physionet.org database (https://physionet.org/content/eegmat/1.0.0/). It includes EEG and ECG recordings sampled at $500Hz$ from healthy individuals performing mental arithmetic tasks (i.e. mentally adding and subtracting integers). Each recording features a 180-second resting period followed by a 60-second mental arithmetic task (MA).

Individuals with normal or corrected-to-normal visual acuity, normal color vision, and no signs of mental or cognitive impairment or learning disabilities were eligible to participate in the study. Exclusion criteria included the use of psychoactive drugs, addiction to drugs or alcohol, and any neurological or psychiatric issues.

The experiment involved 36 volunteers, with data from 32 of them (24 female) being retained for further processing after a visual inspection analysis was performed to identify gross artifacts. The average age of participants was 18.125 y/o with a standard deviation of 2.01 y/o.

In this study, artifacts such as ocular, muscular, and cardiac on EEG series were detected using a power line notch filter at 50 Hz and a $[0.5-45]$ Hz band-pass filter, followed by independent component analysis. The preprocessing details of the EEG signal acquisition can be found in [14]. The power spectral density (PSD) of the EEG series was estimated through the implementation of the short-time Fourier transform, with a Hamming window of 2000 samples (2 seconds) and a 95% overlap. The PSD was then integrated into the α $(8-12$ Hz) and β $(12-30$ Hz) frequency bands.

For ECG analysis, the Pan-Tompkins algorithm [15] was used to identify the R-peaks and derive HRV series. The series were further examined for any potential artifacts using Kubios HRV software. The HRV series were interpolated and sampled at 4 Hz. The Smoothed Pseudo Wigner-Ville Distribution (SPWVD) method [16] was utilized to obtain a time-frequency representation, due to its low variance and independent control over filtering in both temporal and frequency domains. The obtained PSD estimation was integrated into the low frequency (LF: $[0.04-0.15$ Hz$]$) and high frequency (HF: $[0.15-0.4$ Hz$]$) bands of interest.

B. Brain-Heart Interplay estimation

The synthetic data generation (SDG) model was used to quantify the functional directional brain-heart interaction (BHI), as described in detail in [17], [18]. The SDG model consists of two coupled systems that generate synthetic heartbeat and brain activity data. On the brain side, synthetic EEG is generated through a combination of oscillators, while the heart-to-brain interaction is modeled through an exogenous term in an exogenous autoregressive model of the first order. On the heartbeat side, a synthetic HRV series is produced by an integral pulse frequency modulation model, with parameters influenced by EEG activity, representing the functional BHI.

To estimate time-varying BHI across HRV-LF and HF bands and various EEG frequency ranges, the SDG model was fitted to experimental EEG and HRV power spectral density (PSD) series. The resulting BHI series have the same time resolution as the PSD series.

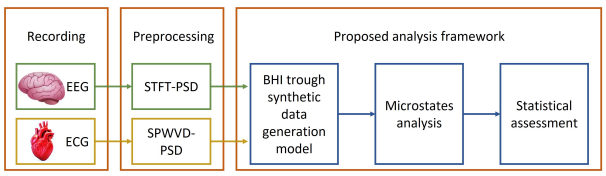

Fig. 1: Blocks diagram of the analysis procedure implemented.

C. Microstate Analysis

The standard method for identifying and extracting microstates from typical EEG activity was partially utilized in this study, as described in detail in [1]. The MATLAB toolbox used in this study, which is freely downloadable, is described in [19].

In order to estimate BHI microstates, the method was adapted for this study. Firstly, topographic maps of the BHI-GFP, the BHI equivalent of the EEG-derived global field potential (GFP), were constructed. As the EEG-GFP corresponds to the spatial standard deviation [20], which estimates the time-resolved amount of activity accounting for the data of all EEG electrodes, the BHI-GFP corresponds to the spatial standard deviation of BHI, which estimates the time-resolved amount of BHI accounting for the data of all EEG electrodes.

The BHI-GFP peaks were identified and used for segmentation, and a modified k-means algorithm was used for clustering. A meta-criterion based on a trade-off between various fit measures (global explained variance, cross-validation criterion, Krzanowski-Lai criterion, and dispersion) was used to determine the number of BHI microstates, and the identified topographies were evaluated for plausibility.

Once the microstate prototypes were selected, they were fitted to the entire BHI series. Each BHI topographical sample was matched to a particular microstate prototype based on its degree of similarity. The goodness of fit was evaluated through the global explained variance (GEV), which measures how much of the original GFP dynamics variance is explained by the microstate time series. To ensure continuity, a smoothing operation with a smoothing window of 250 ms with no overlap was eventually applied [19]. The topographical smoothness and continuity of the extracted prototypes are commonly used to evaluate their physiological plausibility.

III. Experimental Results

In this study, three BHI microstates were identified for each combination of BHI direction and frequency band, i.e., $C_{brain_b \to heart_b}$ and $C_{heart_b \to brain_b}$, where $brain_b$ refers to the EEG-derived α or β bands and $heart_b$ stands for HRV-derived low frequency (LF) or high frequency (HF) bands.

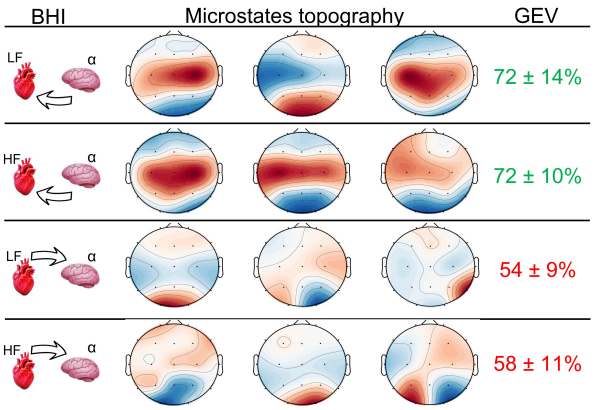

Fig. 2: Experimental results for EEG-derived α band. The left column indicates the direction of BHI (brain-to-heart or heart-to-brain) and the HRV frequency band (LF and HF) involved. The right column displays the median global explained variance (GEV) across subjects with standard deviation, calculated through the backfitting operation on the microstate prototypes, shown in the central part of the figure.

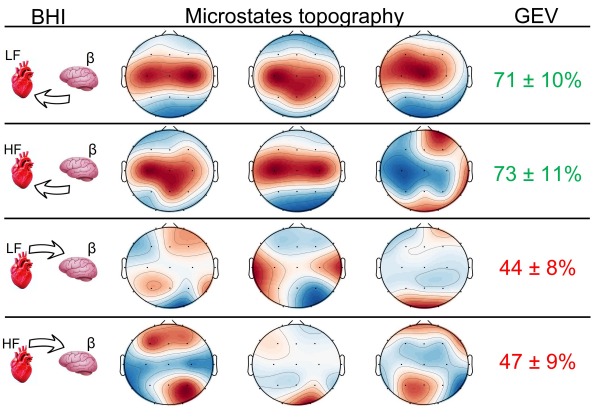

Fig. 3: Experimental results for EEG-derived β band. The left column shows the direction of BHI (brain-to-heart or heart-to-brain) and HRV-frequency band (LF or HF) involved. The right column displays the median across-subject global explained variance (GEV) $\pm$ standard deviation, obtained from the backfitting operation on the microstate prototypes depicted in the center of the figure.

As shown in Figure 2, the microstate prototypes associated with the EEG-α band have been identified, along with the related GEV. It is intriguing to note that both α-to-heart microstates have a GEV greater than 70%, indicating that the microstate analysis effectively captures the spatiotemporal dynamics of $C_{\alpha\to LF}$ and $C_{\alpha\to HF}$. On the other hand, the GEV is less than 60% for both $C_{LF\to\alpha}$ and $C_{HF\to\alpha}$, meaning that the heart-to-brain dynamics is not well explained by the algorithm.

The topographical representation of the prototypes, as shown in Figure 2, is informative in its own right. The prototypes extracted from $C_{\alpha\to LF}$ and $C_{\alpha\to HF}$ (i.e., from brain-to-heart direction) have a smooth and physiologically plausible distribution, while those extracted from $C_{LF\to\alpha}$ and $C_{HF\to\alpha}$ (i.e., from heart-to-brain direction) have a less continuous and more disturbed distribution.

Given the limited GEV and the information provided by the topographies, the heart-to-α BHI microstates were not deemed robust and no further statistical comparisons were performed in that direction.

Experimental results for EEG-β bands are displayed in Figure 3, which mirrors the structure of Figure 2. In line with the results obtained from the α band, the GEV for β-to-heart microstates is greater than 70% while the GEV for heart-to-β is less than 50% for both LF and HF HRV oscillations. Additionally, prototypes extracted from $C_{\beta\to LF}$ and $C_{\beta\to HF}$ exhibit a continuous and physiological distribution, in contrast to those extracted from $C_{LF\to\beta}$ and $C_{HF\to\beta}$. These results from α and β EEG components are consistent and indicate that microstate representation does not robustly explain heart-to-brain BHI dynamics.

Figure 4 displays the frequency of each microstate (f_M), normalized per window's length, for participants under two experimental conditions. Each subpanel corresponds to a different EEG- or HRV- frequency band and presents results for both resting state and mental arithmetic tasks. This figure demonstrates the change in BHI microstate distribution with experimental conditions. For example, in the top-left panel, which refers to $C_{\alpha\to LF}$ microstates, the second microstate prototype experiences a significant decrease in frequency from the resting state to mental arithmetic task, while the third prototype, which had a minor frequency during the resting state, increases in frequency during the mental arithmetic task. Other changes are also detected. A χ^2 test for contingency tables, implemented on a 3×2 contingency table (one for each combination of EEG- and HRV- frequency bands), was performed to determine the significance of these changes, and p-values were always below the significance threshold of 0.01. The test was performed by adding the f_M of each microstate (3 rows) for all subjects, separately for the resting state and mental arithmetic task (2 columns).

IV. Discussions and Conclusion

The aim of the present study was to explore the possibility of extending the concept of EEG microstates to the brain-heart axis. Based on previous research that suggests that brain regions associated with EEG microstates belong to the central autonomic network (CAN) [7]–[9], we hypothesized the existence of brain-heart microstates, which could be identified through the combination of EEG and heartbeat dynamics analysis.

A pipeline was designed to construct a brain-heart interplay (BHI) associated global field power (GFP) starting from an electrode-wise BHI estimation using a synthetic data generation (SDG) model [17]. The obtained BHI signal was then analyzed using EEG microstate analysis to identify the microstate prototypes fitted with the experimental data.

The study used experimental data related to elicited CNS and ANS responses during mental arithmetic tasks. The

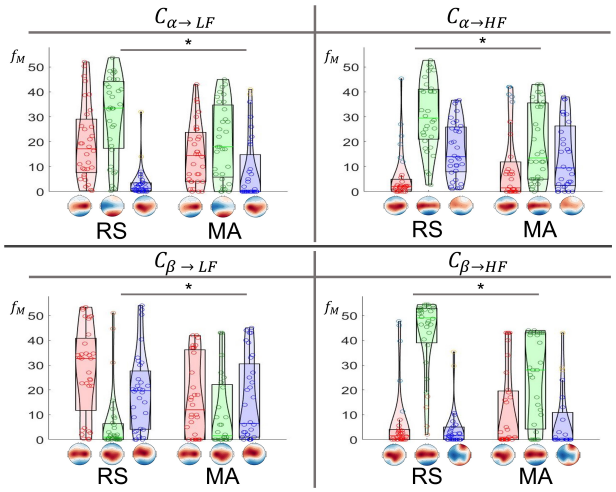

Fig. 4: Boxplots statistics showing the normalized frequency (f_M) of each microstate per unit of window time, for participants under two experimental conditions. Results for $C_{\alpha\rightarrow LF}$ are displayed in the top-left panel, $C_{\beta\rightarrow LF}$ in the bottom-left, $C_{\alpha\rightarrow HF}$ in the top-right panel, and $C_{\beta\rightarrow HF}$ in the bottom-right panel. Each boxplot corresponds to the microstate prototype depicted at its base and results for resting state (RS) are on the left and mental arithmetic task (MA) on the right. An asterisk signifies a statistically significant ($p < 0.01$) difference in microstate distribution.

results revealed a clear asymmetry between the brain-to-heart and heart-to-brain directional BHI systems, with microstate prototypes only being identified in the brain-to-heart direction. Consequently, this study suggests that BHI microstates exist, but only in the descending direction from the brain to the heart. As a matter of fact, BHI is known to be a strongly directional phenomenon, and the discrepancy found in this study could be due to physiological and methodological reasons. Indeed, from one side, BHI mediated by CNS control over ANS activity involves broad brain networks (e.g., CAN and default mode network) [9]. From the other side, previous studies have reported direct CNS reactions to cardiovascular activity (e.g., heartbeat evoked potentials [21]), which could be more localized in the space and time domain [22]. Additionally, microstate analysis might not capture transient localized activity [3]. Thus, the asymmetric identification of BHI-microstates in the brain-to-heart direction only, supports the hypothesis that BHI phenomenon is more diffuse over the scalp in descending direction, and more localized in the ascending one.

The analysis also revealed that mental arithmetic leads to statistically significant changes in the distribution of BHI microstate occurrences.

In conclusion, the present study provides evidence for the existence of microstates of the brain-heart axis, which are spatio-temporal quasi-stable states that only refer to the efferent brain-to-heart direction and change in number and topography under different conditions. This demonstrates that descending brain-heart communication occurs not only at the regional level, but also at the whole-brain level. Future studies will focus on characterizing BHI microstates in different physiological and pathological conditions using different methodologies.

References

[1] C. M. Michel and T. Koenig, "Eeg microstates as a tool for studying the temporal dynamics of whole-brain neuronal networks: a review," *Neuroimage*, vol. 180, pp. 577–593, 2018.

[2] W. Hu *et al.*, "Microstate detection in naturalistic electroencephalography data: A systematic comparison of topographical clustering strategies on an emotional database," *Frontiers in Neuroscience*, vol. 16, 2022.

[3] D. Van de Ville *et al.*, "Eeg microstate sequences in healthy humans at rest reveal scale-free dynamics," *Proceedings of the National Academy of Sciences*, vol. 107, no. 42, pp. 18179–18184, 2010.

[4] S. L. Bressler and V. Menon, "Large-scale brain networks in cognition: emerging methods and principles," *Trends in cognitive sciences*, vol. 14, no. 6, pp. 277–290, 2010.

[5] Y. e. a. Li, "Abnormalities in resting-state eeg microstates are a vulnerability marker of migraine," *The Journal of Headache and Pain*, vol. 23, no. 1, pp. 1–12, 2022.

[6] L. Tait *et al.*, "Eeg microstate complexity for aiding early diagnosis of alzheimers disease," *Scientific reports*, vol. 10, no. 1, pp. 1–10, 2020.

[7] J. Britz *et al.*, "Bold correlates of eeg topography reveal rapid resting-state network dynamics," *Neuroimage*, vol. 52, no. 4, pp. 1162–1170, 2010.

[8] F. Musso *et al.*, "Spontaneous brain activity and eeg microstates. a novel eeg/fmri analysis approach to explore resting-state networks," *Neuroimage*, vol. 52, no. 4, pp. 1149–1161, 2010.

[9] G. Valenza *et al.*, "The central autonomic network at rest: uncovering functional mri correlates of time-varying autonomic outflow," *Neuroimage*, vol. 197, pp. 383–390, 2019.

[10] D. Candia-Rivera, V. Catrambone, J. F. Thayer, C. Gentili, and G. Valenza, "Cardiac sympathetic-vagal activity initiates a functional brain-body response to emotional arousal," *Proceeding of the National Academy of Science*, 2022.

[11] A. Silvani *et al.*, "Brain–heart interactions: physiology and clinical implications," *Philosophical Transactions of the Royal Society A: Mathematical, Physical and Engineering Sciences*, vol. 374, no. 2067, p. 20150181, 2016.

[12] X. Yu *et al.*, "Estimation of the cortico-cortical and brain-heart functional coupling with directed transfer function and corrected conditional entropy," *Biomedical Signal Processing and Control*, vol. 43, pp. 110–116, 2018.

[13] V. Catrambone *et al.*, "Time-resolved brain-to-heart probabilistic information transfer estimation using inhomogeneous point-process models," *IEEE Transactions on Biomedical Engineering*, vol. 68, no. 11, pp. 3366–3374, 2021.

[14] I. Zyma *et al.*, "Electroencephalograms during mental arithmetic task performance," *Data*, vol. 4, no. 1, p. 14, 2019.

[15] J. Pan and W. J. Tompkins, "A real-time qrs detection algorithm," *IEEE transactions on biomedical engineering*, no. 3, pp. 230–236, 1985.

[16] M. Orini *et al.*, "Characterization of dynamic interactions between cardiovascular signals by time-frequency coherence," *IEEE Trans. on Biom. Eng.*, vol. 59, no. 3, pp. 663–673, 2012.

[17] V. Catrambone *et al.*, "Time-resolved directional brain–heart interplay measurement through synthetic data generation models," *Annals of biomedical engineering*, vol. 47, no. 6, pp. 1479–1489, 2019.

[18] V. Catrambone and G. Valenza, *Functional Brain-Heart Interplay: From Physiology to Advanced Methodology of Signal Processing and Modeling*. Springer Nature, 2021.

[19] A. Poulsen *et al.*, "Microstate eeglab toolbox: An introductory guide," *BioRxiv*, p. 289850, 2018.

[20] W. Skrandies, "Global field power and topographic similarity," *Brain topography*, vol. 3, no. 1, pp. 137–141, 1990.

[21] M. Coll *et al.*, "Systematic review and meta-analysis of the relationship between the heartbeat-evoked potential and interoception," *Neuroscience & Biobehavioral Reviews*, vol. 122, pp. 190–200, 2021.

[22] O. Pollatos *et al.*, "Brain structures involved in interoceptive awareness and cardioafferent signal processing: a dipole source localization study," *Human brain mapping*, vol. 26, no. 1, pp. 54–64, 2005.